Journal of Solid State Chemistry **149,** 28–32 (2000)
Article ID jssc.1999.8489, available online at http://www.idealibrary.com on IDEAL®

Inert Pair Effects in Tin and Lead Dihalides: Crystal Structure of Tin(II) Bromide

I. Abrahams[1] and D. Z. Demetriou

Structural Chemistry Group, Department of Chemistry, Queen Mary and Westfield College, Mile End Road, London E1 4NS, United Kingdom

Received April 19, 1999; in revised form August 11, 1999; accepted August 27, 1999

The crystal structure of stannous bromide, $SnBr_2$, is compared with those of its analogs: $SnCl_2$, $PbBr_2$, and $PbCl_2$. The structure of $SnBr_2$ has been refined by Rietveld analysis of X-ray powder diffraction data in the orthorhombic space group *Pbnm*, with $a = 10.5251(7)$ Å, $b = 8.3936(5)$ Å, $c = 4.2369(2)$ Å, and $Z = 4$. Refinement terminated with $R_{wp} = 11.90\%$ and $R_{ex} = 19.11\%$. Sn is in a trigonal-pyramidal coordination with three Br atoms, two of which are bridging and one terminal. The bridging units form polymeric chains, which run parallel to the *c*-axis. $SnBr_2$ is related to, but is not isostructural with, analogs, $PbCl_2$, $PbBr_2$, and $SnCl_2$. All the structures possess $(MX_2)_n$ chains (M = Sn or Pb, X = Cl or Br), but those in $SnBr_2$ are shifted with respect to each other, resulting in a difference in the secondary M–X coordination shell. Stereochemical distortions caused by the nonbonding valence electron pairs on the metal atoms are compared using unit cell parameters normalized to take into account differences in covalent radii between the structures. © 2000 Academic Press

INTRODUCTION

The structures of Sn(II) and Pb(II) are often characterized by stereochemical distortion caused by the nonbonding valence electrons of the metal atom. In Sn(II) compounds, the most common metal environment is a trigonal-pyramidal arrangement of nearest neighbors with three more distant tin–ligand contacts completing a distorted octahedral environment, as, for example, in $NH_4Br \cdot NH_4SnBr_3 \cdot H_2O$ (1), where $[SnBr_3]^-$ units are found as essentially discrete anions. In other tin(II) bromide systems, interactions between the nonbonding valence electrons on tin and low-lying empty Br4*d* orbitals result in stabilization of certain structures, as is seen in $Cs_2Sn_6Br_3F_{11}$ (2). In some cases, these interactions can lead to the complete removal of stereochemical distortion through electronic population of low-lying conduction bands, as in $CsSnBr_3$ (3).

$SnBr_2$ is a classic compound of divalent tin and is an important reagent in both inorganic and organic synthetic chemistry. The analogs $SnCl_2$ (4), $PbCl_2$ (5, 6), and $PbBr_2$ (6) are essentially isostructural with each other (note the published data on $SnCl_2$ are related to those of $PbCl_2$ by an origin shift of half a unit cell in the longest axial dimension). Indeed, $PbCl_2$ and $PbBr_2$ form a complete solid solution range, some members of which show relatively high ionic conductivity (6). One might expect $SnBr_2$ to have a structure similar to that of its analogs. However, an early work by Andersson (7) suggested structural differences between lead(II) and tin(II) bromides. In that study "approximate" atomic positions were given for $SnBr_2$. To clarify the structural relationship between $SnBr_2$ and its analogs, we have investigated its structure by X-ray powder diffraction.

[1]To whom correspondence should be addressed. E-mail: I.Abrahams@qmw.ac.uk.

EXPERIMENTAL

Preparation

$SnBr_2$ was prepared by heating metallic tin with hydrobromic acid under reflux. All operations were carried out under N_2. Hydrobromic acid (200 cm^3) was added to granulated tin (100 g) and the mixture heated under reflux until most of the tin had dissolved. The solution was decanted into a beaker and heated to evaporate excess HBr. The resulting yellow solid was strongly heated until melting occurred. The red liquid cooled to yield a white solid. Titrimetric Sn(II) analysis (8) gave Sn 41.2% (42.6% calculated).

X-Ray Diffraction

X-ray powder diffraction data were collected on a Stoe STADI/P high-resolution diffractometer in symmetric transmission geometry using Ge-monochromated Cu$K\alpha_1$ radiation ($\lambda = 1.54056$ Å). Data were acquired between 5 and 85° 2θ, at intervals of 0.02°, using a small linear position sensitive detector. Calibration was with an external Si standard. A transmission absorption correction was applied to the data prior to refinement. The crystal structure of $SnBr_2$ was refined by the Rietveld method, with the program GSAS (9), in the orthorhombic space group *Pbnm* (No.

0022-4596/00 $35.00

62 (10)). Crystal and refinement parameters are summarized in Table 1. The atomic parameters used in the initial model were based on the approximate positions suggested by Andersson (7). Peak shapes were modeled on a pseudo-Voigt distribution, with scattering factors for neutral atoms assumed. Isotropic thermal parameters were refined for all atoms and a small preferred orientation correction refined in the 100 direction. Unit cell projections were obtained with PLUTON (11). The final refined parameters are presented in Table 2, with the corresponding fitted profile in Fig. 1. Significant contact distances and angles are presented in Table 3.

TABLE 1
Crystal and Structure Refinement Data for $SnBr_2$

(a) Crystal data	
Name	Tin(II) bromide
Empirical formula	$SnBr_2$
Structural formula	$(SnBr_2)_n$
Formula weight	278.498
Crystal system	Orthorhombic
Space group	*Pbnm* (No. 62)
Unit cell dimensions	$a = 10.5251$ (7), $b = 8.3936(5)$, $c = 4.2369(2)$ Å
Volume	374.30(6) Å^3
Z	4
Density (calculated)	4.944 g cm^{-3}
Absorption coefficient μ	77.16 mm^{-1}
$F(000)$	480
Sample description	White powder
Synthesis	Reflux of metallic Sn in HBr
(b) Refinement	
Refinement software	GSAS (9)
Initial model source	$SnBr_2$ (7)
2θ range refined	10–85°
Data corrections	Transmission absorption correction; preferred orientation on 100
Number of observations/restraints parameters	3738/0/34
Total number of reflections used	160
Peak shape	Pseudo-Voigt
Final R-factors[a]	$R_p = 0.0925$, $R_{wp} = 0.1190$ $R_{ex} = 0.1911$, $\chi^2 = 0.3909$ $R_{F^2} = 0.2139$
Maximum atomic shift/esd	< 0.01

[a]For definition of R-factors, see Ref. 17.

TABLE 2
Atomic Coordinates and Isotropic Thermal Parameters for $SnBr_2$

Atom	Site	x	y	z	Occupancy	U_{iso}(Å^2)
Sn	4*c*	0.3288(3)	0.3662(3)	0.25(–)	1.0(–)	0.035(2)
Br(1)	4*c*	0.1787(5)	0.5139(5)	0.75(–)	1.0(–)	0.026(2)
Br(2)	4*c*	0.4501(4)	0.6650(5)	0.25(–)	1.0(–)	0.015(2)

RESULTS AND DISCUSSION

A projection of the crystal structure of $SnBr_2$ is shown in Fig. 2. Sn is in essentially trigonal-pyramidal geometry, with three short Sn–Br bonds less than 3 Å. Two bonds at 2.92 Å are to bridging Br(1) atoms, while one bond at 2.81 Å is to a terminal Br(2). These bond lengths can be compared with the average of 2.71 Å found for the discrete $[SnBr_3]^-$ anion (1). The trigonal pyramids corner share to give polymeric chains of $[SnBr_2]_n$ which run parallel to the *c*-axis vector. In each chain the pyramids are arranged such that the nonbonding valence electrons on the tin atoms all point in the same direction between the chains. Adjacent chains have pyramids orientated in opposite directions. A further three contacts to Br, above 3.1 Å, complete a distorted octahedral environment. The nonbonding valence electrons are clearly stereochemically active, preventing a more regular octahedral coordination geometry.

The structure of $SnBr_2$ is related to those of $PbBr_2$ (6), $SnCl_2$ (4), and $PbCl_2$ (5, 6). Despite an apparent similarity in unit cell dimensions and space group with these structures, $SnBr_2$ is not isostructural, but is clearly related. All the structures contain $(MX_2)_n$ polymeric chains (where M = Sn or Pb and X = Br or Cl) running parallel to the *c*-axis vector; however, the relative positions of the MX_2 units between chains is different in the present structure. Fig. 3a shows a projection down the *b*-axis of $SnBr_2$, while Fig. 3b shows the same projection for the $PbBr_2$ structure. It can clearly be seen that the chains in $SnBr_2$ are shifted by half a unit cell in the *c*-axis direction with respect to each other when compared with the analogous chains in $PbBr_2$. This leads to a difference in the secondary Br coordination shell for Sn when compared with Pb. The orientation of the chains is also different in $SnBr_2$.

Table 4 shows a comparison of contact distances between $SnBr_2$ and its analogs. It is clear that the difference in orientation of the $(MX_2)_n$ chains leads to a difference in the secondary halide coordination shell of the metal atom. In $PbBr_2$, $SnCl_2$, and $PbCl_2$, four noncovalent contacts to neighboring Br atoms are seen under 3.4 Å, whereas in $SnBr_2$ only three noncovalent Sn–Br contacts are seen in this range, with the next nearest contacts significantly higher at 3.639(4) Å to two Br(1) atoms. A measure of the size and stereochemical activity of the nonbonding valence electron pairs on the metal atoms is the difference between the average contact distances in the first and second coordination shells (Table 5). The largest difference occurs in $SnCl_2$, suggesting that the inert pair orbitals in this structure exhibit the most repulsion. $SnBr_2$ has a smaller difference value than $SnCl_2$, suggesting a lesser degree of repulsion. ^{119}Sn Mössbauer spectroscopic data (12) on $SnBr_2$ and

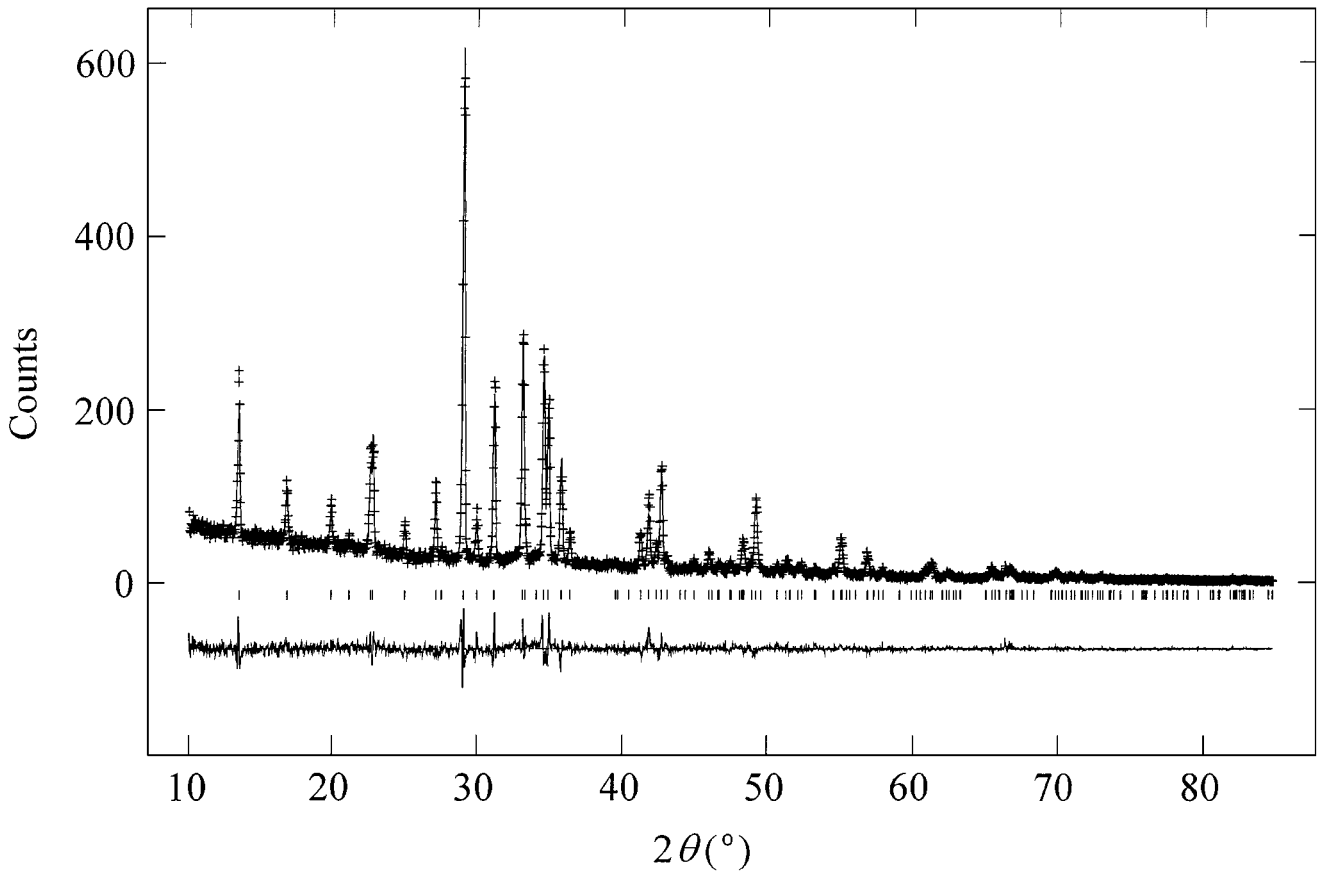

FIG. 1. Final fitted X-ray diffraction profile for $SnBr_2$, showing observed (points), calculated (line), and difference (lower) profiles. Markers indicate the reflection positions.

$SnCl_2$, with chemical shifts of $\delta = 1.93(5)$ and 2.07(5) mm s^{-1} (referenced to α-Sn), respectively, indicate a slightly greater *s* electron density at the Sn nucleus in $SnCl_2$ than $SnBr_2$. This suggests more directional (*p* orbital) character in the inert pair orbital in $SnCl_2$ and hence a greater repulsive force for this orbital. The two lead compounds have similar levels of distortion, with lower difference values than the tin analogs, reflecting the generally found observation that Pb(II) structures show a lesser degree of distortion due to inert pair effects than Sn(II) analogs. The metal nucleus to inert pair distances have been calculated as 0.95 Å for Sn^{2+} and 0.86 Å for Pb^{2+} (13). This contraction of the inert pair

TABLE 3
Significant Contact Distances (Å) and Angles (°) for $SnBr_2$[a]

$Sn–Br(1)_{a,b}$	$2.919(4) \times 2$	$Sn–Br(2)_a$	2.814(5)
$Sn–Br(2)_{c,d}$	$3.158(4) \times 2$	$Sn–Br(2)_e$	3.387(5)
$Sn \cdots Sn_{b,f}$	$4.237(1) \times 2$		
$Br(1)_a–Sn–Br(1)_b$	93.1(2)	$Br(1)_{a,b}–Sn–Br(2)_a$	$82.4(1) \times 2$
$Br(1)_{a,b}–Sn–Br(2)_{c,d}$	$157.1(2) \times 2$	$Br(1)_{a,b}–Sn–Br(2)_{d,c}$	$87.0(1) \times 2$
$Br(1)_{a,b}–Sn–Br(2)_e$	$75.1(1) \times 2$	$Br(2)_a–Sn–Br(2)_{c,d}$	$74.9(1) \times 2$
$Br(2)_a–Sn–Br(2)_e$	146.9(2)	$Br(2)_c–Sn–Br(2)_d$	84.3(1)
$Br(2)_{c,d}–Sn–Br(2)_e$	$126.7(1) \times 2$	$Sn–Br(1)_{a,b}–Sn_{f,b}$	93.1(2)

[a]Symmetry relationships: (a) x, y, z; (b) $x, y, z-1$; (*c*) $1-x, 1-y, -z$; (d) $1-x, 1-y, 1-z$; (e) $0.5-x, y-0.5, z$; (f) $x, y, 1+z$.

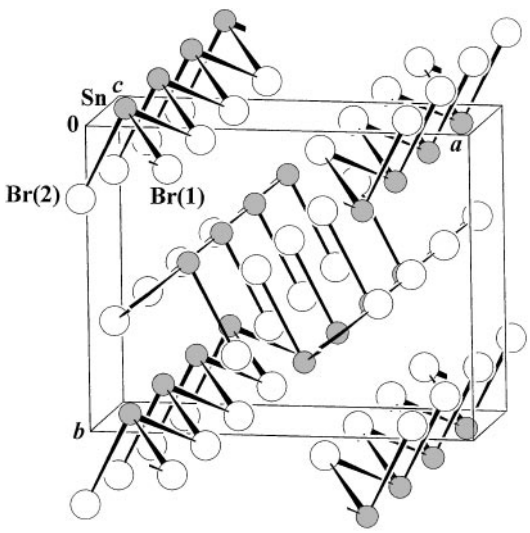

FIG. 2. Unit cell projection of the structure of $SnBr_2$. Shaded and unshaded circles represent Sn and Br atoms, respectively.

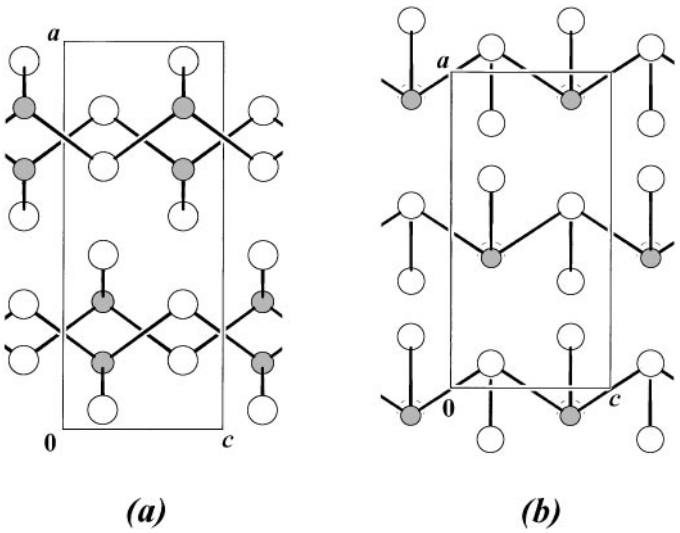

FIG. 3. Projection down the *b*-axis of (a) $SnBr_2$ and (b) $PbBr_2$. Shaded and unshaded circles represent Sn/Pb and Br atoms, respectively. Note that the *a*- and *b*-axes have been transposed from Ref. 6 to correspond to the same space group setting as in the present work and that (a) and (b) are not to the same scale.

orbital in descending periods has been explained in terms of relativistic contractions (14, 15), with the *s* electrons in the 6*s* shell being more strongly bound (i.e., higher binding energies) than those in the 5*s* shell.

The difference in the raw unit cell volumes between the structures (Table 5) reflects not only the difference in repulsion caused by the stereochemically active inert pairs on the metal atoms but also the difference in size of the atoms. To allow direct comparison of distortion effects, the unit cell parameters can be normalized with respect to the sum of the Pb and Br covalent radii. The normalization therefore accounts for differences in the atom sizes. A normalization matrix can be applied to the unit cell parameters as follows:

$$\begin{pmatrix} a_{\text{norm}} \\ b_{\text{norm}} \\ c_{\text{norm}} \end{pmatrix} = \begin{pmatrix} f_{MX} & 0 & 0 \\ 0 & f_{MX} & 0 \\ 0 & 0 & f_{MX} \end{pmatrix} \begin{pmatrix} a \\ b \\ c \end{pmatrix}.$$

f_{MX} is a normalization factor for compound MX_2 and is given by

$$f_{MX} = l_{\text{PbBr}}/l_{MX},$$

where l_{MX} is the sum of the covalent radii for atoms *M* and *X*, and l_{PbBr} is the sum of the covalent radii for Pb and Br, with covalent radii taken as Sn, 1.40 Å; Pb, 1.54 Å; Br, 1.142 Å; and Cl, 0.99 Å (16). Normalized volumes were calculated with the unit cell data for $SnBr_2$, $SnCl_2$ (4), $PbBr_2$ (6), and $PbCl_2$ (5) (Table 5). The normalized volumes for $PbCl_2$ and $PbBr_2$ are similar and suggest similar degrees of stereochemical activity in these compounds. There is a large increase in normalized volume on changing the metal atom from Pb to Sn, with the two tin compounds having similar normalized volumes. This is consistent with greater repulsion from the Sn inert pair orbitals compared to those of Pb.

As the $(MX_2)_n$ chains run parallel to the *c*-axes in each of the structures, the areas of the perpendicular *a*/*b* cell planes give an indication of the relative chain separation. It is clear that the general trend seen in the differences between primary and secondary coordination shells is reflected in that of the normalized *a*/*b* plane areas. The two lead compounds have similar normalized plane areas, whereas those for the two tin compounds are significantly higher. Unlike their normalized volumes, the normalized *a*/*b* plane area for $SnBr_2$ is higher than that for $SnCl_2$. This high value for $SnBr_2$ is related to the *c*-axis shift between chains discussed above, which results in a greater separation between chains than would be expected if the $SnCl_2$ structure was maintained in $SnBr_2$.

The reasons for $SnBr_2$ adopting a different but related structure to its analogs are unclear. The *X*–*M*–*X* bond angles in the $SnBr_3$ trigonal prism in $SnBr_2$ are more regular than those found in its analogs (105.6, 79.9° × 2 in $SnCl_2$ (4); 103.3, 76.6° × 2 in $PbBr_2$ (6); and 103.5, 75.5° × 2 in $PbCl_2$ (5)) and are close to those found in the free $[SnBr_3]^-$ anion (91.1, 88.3, and 91.3°) in the solid state (1). Clearly, in the case of $SnBr_2$, the more regular coordination geometry around the metal atom is thermodynamically favored over that which would result from adoption of the $SnCl_2$ structure.

TABLE 4
Comparison of *M*–*X* Contact Distances (Å) under 3.5 Å in MX_2 Compounds (*M* = Sn or Pb, *X* = Br or Cl)

	Primary coordination shell			Secondary coordination shell				
Compound	*M*–*X*(1)	*M*–*X*(2)	*M*–*X*(3)	*M*–*X*(4)	*M*–*X*(5)	*M*–*X*(6)	*M*–*X*(7)	Ref.
$SnBr_2$	2.814	2.919	2.919	3.158	3.158	3.387	–	This work
$SnCl_2$	2.664	2.782	2.782	3.058	3.058	3.219	3.302	4
$PbBr_2$	2.954	3.017	3.017	3.205	3.205	3.269	3.290	6
$PbCl_2$	2.850	2.873	2.873	3.067	3.072	3.072	3.076	5

TABLE 5
Comparison of Structural Parameters for MX_2 Compounds (M = Sn or Pb, X = Br or Cl)

Compound	$\bar{l}_2 - \bar{l}_1$ (Å)[a]	V (Å^3)	V_{norm}(Å^3)	a/b (Å^2)	a_{norm}/b_{norm} (Å^2)
$SnBr_2$	0.35	374.30	445.79	88.34	99.26
$SnCl_2$	0.42	317.85	446.60	71.75	90.00
$PbBr_2$	0.25	363.80	363.80	76.88	76.88
$PbCl_2$	0.21	310.12	369.37	68.70	77.19

[a] $\bar{l}_1$ is the average of the primary coordination shell contacts around M and $\bar{l}_2$ is the average of the secondary coordination shell contacts around M.

ACKNOWLEDGMENT

We thank Dr. P. Lightfoot at the University of St. Andrews for access to high-resolution X-ray data collection facilities.

REFERENCES

1. L. Abrahams, M. Christoforu, S. M. Grimes, and J. D. Donaldson, *J. Chem. Res.* (*M*) 318 (1994).
2. I. Abrahams, J. D. Donaldson, and S. M. Grimes, *J. Chem. Soc., Dalton Trans.* 669 (1992).
3. J. D. Donaldson, J. Silver, S. Hadjiminolis, and S. D. Ross, *J. Chem. Soc., Dalton Trans.* 1500 (1975).
4. J. M. van den Berg, *Acta Crystallogr.* **14,** 1002 (1961).
5. Yu. Z. Nozik, L. E. Fykin, and L. A. Muradyan, *Kristallografiya* **21,** 76 (1976).
6. M. Lumbreras, J. Protas, S. Jebbari, G. J. Dirksen, and J. Schoonman, *Solid State Ionics* **20,** 295 (1986).
7. J. Andersson, *Acta Chem. Scand.* **A29,** 956 (1975).
8. J. D. Donaldson and W. Moser, *Analyst* **84,** 10 (1959).
9. A. C. Larson, R. B. Von Dreele, and M. Lujan, Jr., "GSAS—Generalized Crystal Structure Analysis System". Neutron Scattering Center, Los Alamos National Laboratory, Los Alamcs, NM, 1990.
10. "International Tables for Crystallography" (T. Hahn, Ed.), 3rd ed., Vol. A. Kluwer, Dordrecht, Holland, 1992.
11. A. L. Spek, *Acta Crystallogr.* **A46,** C34 (1990).
12. J. D. Donaldson and D. G. Nicholson, *J. Chem. Soc. A* 145 (1970).
13. B. G. Hyde and S. Andersson, *in* "Inorganic Crystal Structures," p. 259. J. Wiley, New York, 1989.
14. K. S. Pitzer, *Acc. Chem. Res.* **12,** 271 (1979).
15. P. Pyykko and J.-P. Desclaux, *Acc. Chem. Res.* **12,** 276 (1979).
16. J. Emsley, "The Elements." Oxford Univ. Press, New York, 1989.
17. R. A. Young (Ed.), *in* "The Rietveld Method" (IUCR Monographs on Crystallography 5), p. 21. Oxford Univ. Press, New York, 1993.